

## Review

## DNA-guided self-assembly in living cells

Jinqiao Liu,<sup>1,4</sup> Jianpu Tang,<sup>1,4</sup> Zhaobin Tong,<sup>1,4</sup> Guangshuai Teng,<sup>3,4</sup> and Dayong Yang<sup>1,2,\*</sup>

## SUMMARY

Self-assembly processes exist widely in life systems and play essential roles in maintaining life activities. It is promising to explore the molecular fundamentals and mechanisms of life systems through artificially constructing self-assembly systems in living cells. As an excellent self-assembly construction material, deoxyribonucleic acid (DNA) has been widely used to achieve the precise construction of self-assembly systems in living cells. This review focuses on the recent progress of DNA-guided intracellular self-assembly. First, the methods of intracellular DNA self-assembly based on the conformational transition of DNA are summarized, including complementary base pairing, the formation of G-quadruplex/i-motif, and the specific recognition of DNA aptamer. Next, The applications of DNA-guided intracellular self-assembly on the detection of intracellular biomolecules and the regulation of cell behaviors are introduced, and the molecular design of DNA in the self-assembly systems is discussed in detail. Ultimately, the challenges and opportunities of DNA-guided intracellular self-assembly are commented.

## INTRODUCTION

Self-assembly is the process that structural units spontaneously come together to form more ordered and stable structures.<sup>1,2</sup> There are full of self-assembly processes in cells to maintain cellular activities. Particularly, the self-assembly of biological macromolecules, such as nucleic acids, lipids, and proteins, achieves the precise formation of highly ordered structures in complex cellular environments.<sup>3</sup> These structures of self-assembly provide a suitable environment for metabolic reactions and also prevent the adverse interference between biochemical reactions, which is the important material basis of life metabolism.<sup>4</sup> Consequently, observing and simulating the self-assembly processes of biological macromolecules in living cells are conducive to investigating the mechanism of cell behaviors and the principle of drug action at the molecular level, so as to study the artificial regulation of cell metabolism and provide new ideas for disease treatment at subcellular level.<sup>5,6</sup>

Biomacromolecules are ideal materials for the study of intracellular self-assembly due to their good biocompatibility. Scientists have developed several biological macromolecules as materials to build self-assembly systems in living cells, such as polypeptides,<sup>16–21</sup> deoxyribonucleic acid (DNA)<sup>22</sup> and ribonucleic acid (RNA).<sup>23</sup> The self-assembly behaviors of peptides in living cells were usually accomplished through hydrophobic interactions among their amino acid residues. Schreiber et al.<sup>16</sup> utilized *Escherichia coli* as host organism to synthesize amphiphilic peptides through gene regulation. The amphiphilic proteins were self-assembled based on their hydrophilic and hydrophobic properties, resulting in the formation of distinct regions in bacteria. The self-assembly behaviors of nucleic acids in living cells were usually through hydrogen bonding. Aldaye et al.<sup>23</sup> designed an assembly module of RNA, which achieved self-assembly in hydrogen-producing engineering bacteria by forming hydrogen bonds between RNA bases. This RNA self-assembly regulated the distribution of hydrogen-producing-related proteins in bacteria, and successfully improved the efficiency of hydrogen production.

Recently, with the rapid development of DNA nanotechnology, DNA has shown great competitiveness in the construction of intracellular self-assembly systems due to its programmable sequence, predictable nanostructure, and designable functions.<sup>24</sup> On the other hand, the technologies of DNA synthesis are more mature, and the DNA strands of any desired sequence can be synthesized through established chemical synthesis methods, which lays the solid foundations of DNA as an ideal material for intracellular self-assembly. In addition, some DNA molecules with specific sequences have been proven to possess responsiveness toward special stimuli with high sensitivity, such as pH, proteins and metal ions, which makes the methods of DNA-guided

<sup>1</sup>Frontiers Science Center for Synthetic Biology, Key Laboratory of Systems Bioengineering (MOE), Institute of Biomolecular and Biomedical Engineering, School of Chemical Engineering and Technology, Tianjin University, Tianjin 300350, P.R. China

<sup>2</sup>Zhejiang Institute of Tianjin University, Ningbo, Zhejiang 315200, P.R. China

<sup>3</sup>Second Hospital of Tianjin Medical University, Tianjin 300211, P.R. China

<sup>4</sup>These authors contributed equally

\*Correspondence:

dayong.yang@tju.edu.cn

<https://doi.org/10.1016/j.isci.2023.106620>



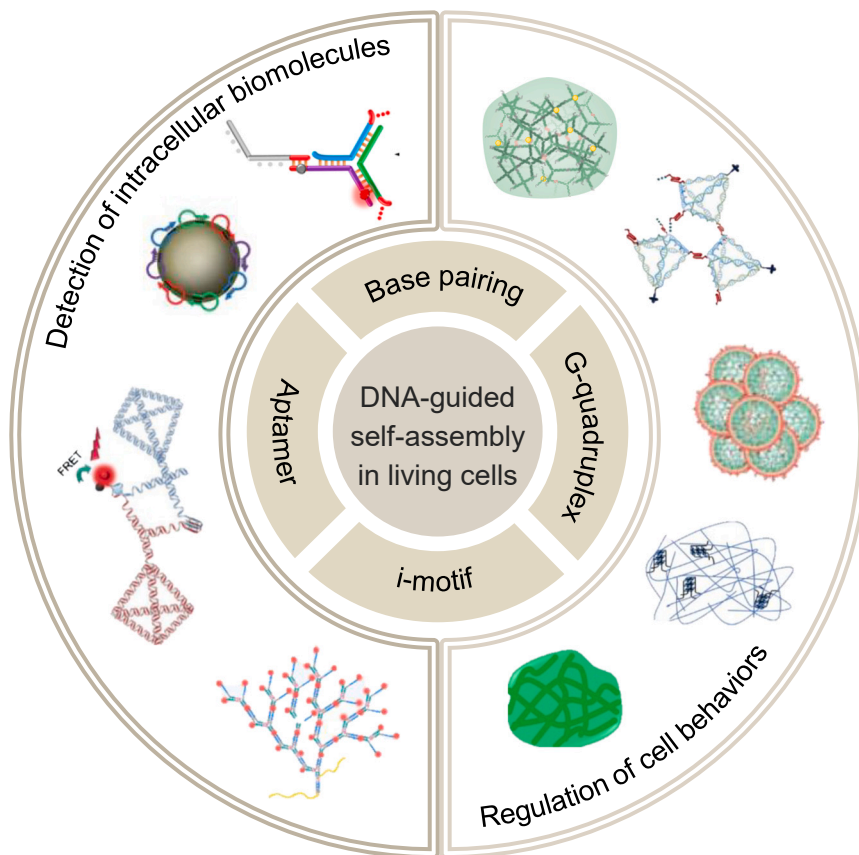


**Figure 1. DNA-guided self-assembly in living cells**

Based on precise sequence design, the methods of DNA self-assembly included complementary base pairing, the formation of G-quadruplet/i-motif structures, and the specific recognition of DNA aptamer. The detection of intracellular biomolecules and the regulation of cell behaviors were accomplished through DNA self-assembly in living cells. Reprinted and adapted with permission from ref.<sup>7-15</sup>

intracellular self-assembly more diverse and intelligent.<sup>25</sup> By integrating these specific DNA sequences in systems, the self-assembly process can be accurately predicted according to the conditions of the intracellular environment, thus building the envisioned DNA self-assemblers in cells or on subcellular structures.<sup>26,27</sup> In this review, we focus on the recent research on DNA-guided intracellular self-assembly and discuss the methods and applications of intracellular self-assembly. The methods of self-assembly are divided according to the conformational transition types of DNA molecules. The applications based on DNA-guided intracellular self-assembly are summarized into the detection of intracellular biomolecules and the regulation of cell behaviors, and the design mechanism of self-assembly systems is discussed in detail (Figure 1).

## METHODS OF SELF-ASSEMBLY

The fundamental monomer of DNA was nucleotide, which consisted of three parts: base (cytosine [C], guanine [G], adenine [A], or thymine [T]), deoxyribose, and phosphate group. According to the principle of Watson-Crick complementary base pairing, single-stranded DNA (ssDNA) self-assembled into double-helix structure mainly by forming two hydrogen bonds between A and T, and three hydrogen bonds between C and G. Besides double-helix DNA structures, there were a large number of non-double-helix DNA structures that were formed through responding to environmental conditions, such as metal ions, protons, and small molecules. With a deeper understanding of intracellular environments, the responsiveness of DNA molecules had been utilized to enable the specific self-assembly of DNA materials at the subcellular level by responding to the heterogeneity of the cellular environment. According to recent research, the methods of DNA-guided intracellular self-assembly were divided into complementary base pairing, the formation of G-quadruplex, the formation of i-motif structure, and the specific recognition of DNA aptamer (Figure 2).

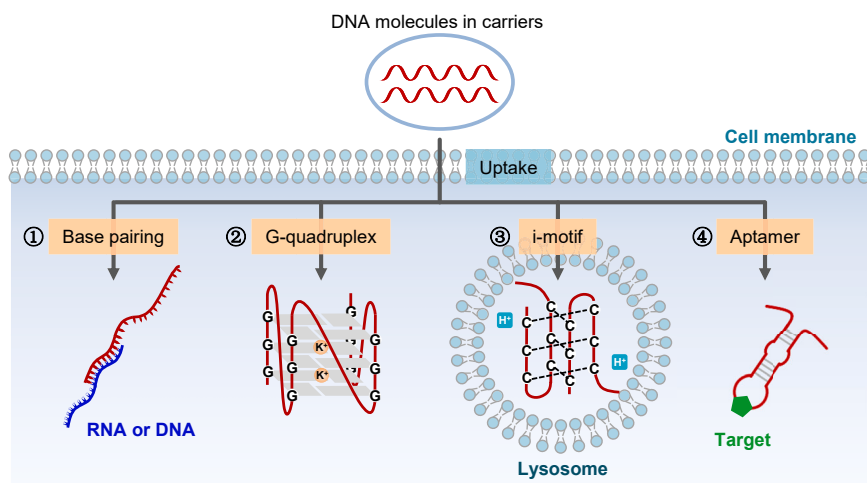


**Figure 2. Methods of DNA-guided self-assembly in living cells, including complementary base pairing, the formation of G-quadruplex/i-motif structure, and the specific recognition of DNA aptamer**

Base complementary pairing, as the most prevalent technique for DNA self-assembly, enabled the rationally designed DNA materials to accurately self-assemble within cells, even in the subcellular structures. Based on complementary base pairing, the single-stranded DNA or RNA, especially that over-expressed in cells, can be utilized as the initiator to trigger the following self-assembly of DNA structural units. Hybridization chain reaction (HCR) was one of the most common strategies based on complementary base pairing for DNA-guided intracellular self-assembly.<sup>28–32</sup> In HCR, the rationally designed hairpin structures, e.g. H1 and H2, were able to coexist stably. When the target DNA (initiator) was present, due to the reaction kinetics and the principle of base complementary pairing, the target DNA and H1 underwent chain replacement reaction to open the hairpin structure of H1 into a chain structure; the sequence in H1 complementary with H2 was exposed to further open H2 into a chain structure; the sequence in H2 complementary with H1 was exposed to promote this reaction to enter the next cycle; finally, a large number of H1-H2 double-stranded complexes were produced. For example, Wu et al.<sup>33</sup> designed the structural units of DNA hairpins to construct nanoscale assemblers, and the DNA hairpins were opened by recognizing the intracellular miRNA, thus triggering HCR. Jin et al.<sup>34</sup> employed graphene oxide as the carrier to deliver DNA hairpins into cancer cells, and HCR was triggered by the RNA on telomerase. Willner et al.<sup>35</sup> developed a method for breast cancer cell imaging and photodynamic therapy by designing the sequences of DNA hairpins for intracellular self-assembly; when these DNA hairpins bound with target miRNA in cells, HCR was activated to expose fluorescent groups, enabling intracellular imaging.

Both G-quadruplex and i-motif were non-double-helix DNA structures. G-quadruplex structure was composed of G-rich DNA strands, and the formation of G-quadruplex relied on the  $\pi$ - $\pi$  stacking between the guanine ring planes and cations, especially potassium ion ( $K^+$ ).<sup>36–38</sup> Consequently, the high concentration of  $K^+$  in cells up to 140 mM was often used to trigger the self-assembly based on G-quadruplex. I-motif structure was formed by C-rich DNA strands with the participation of protons. Protonated cytosine was connected with un-protonated cytosine through hydrogen bonds, and then C-rich DNA strands formed i-motif structures in a reverse parallel way. In cells, C-rich DNA strands were able to form i-motif structures in acidic environments, such as in lysosomes (pH~5.5), which was usually used in the self-assembly based on i-motif.<sup>39,40</sup> For example, Park et al.<sup>41</sup> modified C-rich DNA on gold nanoparticles; after entering lysosomes, the C-rich DNA was induced to form i-motif structures, thus achieving the self-assembly of nanoparticles. The intracellular self-assembly methods guided by the formation G-quadruplex and i-motif depended on the specific chemical environment (proton or metal ion), and can be utilized to achieve DNA self-assembly at the subcellular structures with the same chemical environment.

DNA aptamer was a class of single-stranded oligonucleotide that can form a specific three-dimensional spatial structure and specifically bind to target molecules with high affinity.<sup>42–44</sup> There were many kinds of target molecules discovered to be recognized by DNA aptamer, such as adenosine triphosphate (ATP), amino acids, metal ions, and proteins. In the presence of target molecules, self-assembly can be

achieved by the conformational transition of DNA aptamer and the formation of aptamer-target complex. For example, Li et al.<sup>45</sup> integrated semi-ATP aptamer in branched DNA to achieve self-assembly in intracellular high-level-ATP environments. Gopfrich et al.<sup>46</sup> developed a DNA-based cytoskeleton simulator that enabled the self-assembly of DNA filaments through DNA hybridization and aptamer-ATP interactions, replicating the functions of the natural cytoskeleton. This intracellular self-assembly guided by DNA aptamers depended on specific target molecules in cells, and showed great application potential, especially in the detection of cellular target molecules. However, the screening processes of DNA aptamer for new target molecules were complex, and whether the structure stability of aptamer can support the intracellular self-assembly remained to be verified.

## DETECTION OF INTRACELLULAR BIOMOLECULES

The detection of intracellular biomolecules, especially disease-associated biomarkers, was of great significance in the diagnosis and therapeutic of diseases. However, there were still challenges in achieving the accurate detection of intracellular biomolecules, including the low concentration of target, the demand for real-time monitoring, and the insufficient stability of probes in complex intracellular environments.<sup>47</sup> In recent years, DNA-based probes have been widely investigated in the detection of intracellular biomolecules and presented the advantages in the specific recognition to target and the efficient amplification of signals.<sup>48,49</sup> Herein, several research were introduced on detecting intracellular biomolecules through the rational design of intracellular DNA self-assembly strategy.

Precise complementary base pairing endowed DNA molecules with the remarkable capability of specific recognition of RNA. Recently, a series of probes based on DNA-guided self-assembly had been developed to detect intracellular disease-associated RNA. Survivin mRNA as a type of cancer-associated biomarker has been proven to be abnormally expressed in several cancers, such as colon, lung, prostate, pancreatic, and breast cancers. Li et al.<sup>8</sup> designed four DNA probes with hairpin structures, denoted as H0, H1, H2, and H3, achieving the detection of survivin mRNA in cancer cells through the self-assembly of probes. The zinc oxide nanoparticles (ZnO) coated with polydopamine were used as the carrier to load DNA probes through electrostatic interaction and promote the cell internalization of DNA probes. After uptake by cells, the DNA probes were released into the cytoplasm as the dissolution of ZnO in the acidic environment of lysosomes. Since H0 was designed with higher affinity to bind with survivin mRNA than remaining hairpin structures, H0 was able to specifically recognize the highly expressed survivin mRNA in the cytoplasm and then opened its hairpin structure, which triggered DNA self-assembly through HCR with other three probes (H1, H2, and H3). Since the DNAzyme sequence was integrated into these DNA probes, there were a large number of DNAzyme formed in the DNA assembler. After activation with intracellular  $Mg^{2+}$ , the DNAzyme catalyzed to cut H3, resulting in the release and fluorescence recovery of the fluorophore on H3. By virtue of the efficient self-assembly of DNA probes, the fluorescence signal from survivin mRNA was efficiently amplified. The recovered fluorescence intensity was monitored to detect the relative expression of survivin mRNA in different cell lines, including normal cells (L02, C166, MCF-10A), and cancer cells (HepG2, SMCC-7721, MCF-7). The fluorescence intensities in L02, C166, and MCF-10A cells were significantly lower than that in HepG2, SMCC-7721, and MCF-7 cells, which was consistent with the results of flow cytometry. In addition, the statistical results of fluorescence intensity also showed a consistent trend to the results of survivin mRNA expression measured by quantitative real-time PCR (qRT-PCR), indicating the potential of the DNA probes on the semi-quantitative detection of survivin mRNA.

Thymidine kinase 1 (TK1) messenger RNA (mRNA) was also utilized as the cancer-associated biomarker in diagnosis.<sup>50–52</sup> Zhu et al.<sup>7</sup> developed a self-assembly strategy based on strand replacement reaction between four DNA probes (probe 1, probe 2, assistant 1, and assistant 2), to achieve the detection of TK1 mRNA. They utilized exosomes as a carrier to improve the uptake efficiency of probes by cells. Both probe 1 and probe 2 were composed of two partly complementary single-stranded DNAs (ssDNAs), and the two ssDNAs were separately modified with a fluorophore and a quencher. At the initial state of probes, the fluorescence of fluorophore was quenched; in the presence of target TK1 mRNA, the cyclic self-assembly of four DNA probes was triggered. First, the fluorophore-modified ssDNA of probe 1 would hybridize with TK1 mRNA, and the quencher-modified ssDNA of probe 1 was displaced; the fluorophore-modified ssDNA of probe 1 hybridized with the fluorophore-modified ssDNA of probe 2, and then the quencher-modified ssDNA of probe 2 was displaced; the fluorophore-modified ssDNA of probe 2 then displaced the quencher-modified ssDNA of probe 1 and hybridized with the fluorophore-modified ssDNA of probe 1; all the displaced quencher-modified ssDNA were disabled through hybridizing with assistant 1; finally,

the DNA assembler only composed of fluorophore-modified ssDNA was formed, and fluorescence was efficiently recovered and amplified. By monitoring fluorescence intensity, Zhu et al.<sup>7</sup> verified the feasibility of this strategy in the detection of TK1 mRNA in cells. Since TK1 mRNA was highly expressed in cancer cells (MCF-7, HeLa) compared to normal cells (L02), there was significantly higher fluorescence intensity in MCF-7 and HeLa cells than that in L02 cells, indicating the specificity of this strategy to cancer cell lines and the potential in the detection of intracellular TK1 mRNA.

MicroRNA was a class of endogenous non-coding RNA (about 22 nucleotides) involved in the regulation of protein-coding genes.<sup>53</sup> MicroRNA-21 (miRNA-21) has been proved as an upregulated biomarker in many cancers, and the selective detection of miRNA-21 expression was widely used for early diagnosis of cancer.<sup>54-56</sup> In particular, the visualization of the intracellular distribution of miRNA-21 was crucial for understanding the biological role of miRNA-21 and investigating potential drug targets. Wu et al.<sup>9</sup> developed a strategy based on intracellular self-assembly of the four DNA probes (TH, HA, HB, HC) with hairpin structures, achieving the detection and visualization of miRNA-21 in cancer cells. The two ends of both HC and TH were separately modified by a fluorophore (Cy5/FAM) and a quencher; when HC and TH were in hairpin structures, the Cy5 on HC and the FAM on TH were quenched. Liposome was used as a carrier to deliver DNA probes into the cytoplasm. In the presence of miRNA-21, the self-assembly was triggered; TH recognized miRNA-21 to open its hairpin structure, and the green fluorescence of FAM on TH was recovered due to the weakened quenching effect; the exposure part of TH worked as the initiator of HCR between HA, HB, and HC, to form DNA assembler with nanoscale spherical structure; HCR made the hairpin structure of HC opened, and the red fluorescence of Cy5 on HC was recovered; as HCR process, the TH was displaced from the assembler, and continuously triggered the next HCR, achieving the amplification of fluorescence signal. The nanoscale spherical assembler made it feasible to achieve the intracellular visualization of miRNA-21. Wu et al. set up five groups to verify the efficiency of this strategy, including MCF-7 cells (I), MCF-7 cells treated with estrogen (II, low miRNA-21 expression), MCF-7 cells treated with anti-miR-21D (III, miRNA-21 down-regulation), MCF-7 cells without TH (IV) and L-02 cells (V, negative control group). By fluorescence microscopy imaging, group I showed higher fluorescence intensity than groups II and III, while groups IV and V showed almost no fluorescence, which showed the same trend to miRNA-21 expression in different groups. In addition, the fluorescence of the DNA assembler was used for the spatial location of miRNA-21 at the subcellular level, achieving the real-time visualization of the intracellular distribution of miRNA-21.

DNA-guided intracellular self-assembly had been also utilized to detect the compositions in subcellular structure in real-time. Li et al.<sup>10</sup> developed a self-assembly strategy based on two probes of DNA tetrahedron, achieving the real-time detection of pH and ATP levels in lysosomes (Figure 3A). Both two DNA tetrahedral probes were designed with half i-motif sequences and half ATP aptamer on different vertices. The two probes were separately modified with fluorophore Cy3 and Cy5 on the ends of half ATP aptamer. The two probes were taken up by cells through vesicle-mediated endocytosis. Under the acidic environment of lysosomes, the half i-motif sequences on the two probes formed a complete i-motif structure, achieving the first self-assembly; with the closer distance between two probes, the half ATP aptamer sequences on two probes bound with ATP, achieving the second self-assembly and the formation of DNA assembler (Figure 3A). The second self-assembly made the spatial distance between Cy3 and Cy5 decrease and thus resulted in the quenching of Cy3 due to the fluorescence resonance energy transfer (FRET) from Cy3 to Cy5. Since the efficiency of FRET relied on the concentration of H<sup>+</sup> and ATP, the relative concentration of H<sup>+</sup> and ATP can be detected by monitoring the fluorescence of Cy3 and Cy5. Three groups were set up to investigate the detection efficiency of this strategy, including MCF-7 cells, MCF-7 cells after chloroquine treatment, and MCF-7 cells after oligomycin treatment. Chloroquine was utilized to change the pH in lysosomal to 7.0, thus preventing the formation of i-motif structure; oligomycin was utilized to reduce the ATP concentration in the lysosomes, so that the half ATP aptamer could not recognize ATP. Compared with the MCF-7 cell without treatment, there was a significant decrease in FRET signal after chloroquine and oligomycin treatments (Figure 3B), which demonstrated the feasibility of this DNA self-assembly strategy in the detection of intracellular pH and ATP.

## REGULATION OF CELL BEHAVIORS

The start-up of intracellular DNA self-assembly usually relied on the heterogeneity of physical or chemical factors in the environment, which may lead to the consumption of these factors in the self-assembly process; on the other hand, the formed assembler with a higher-order structure or the introduced functional units in assembler would influence the intracellular environment. Consequently, it has been a promising

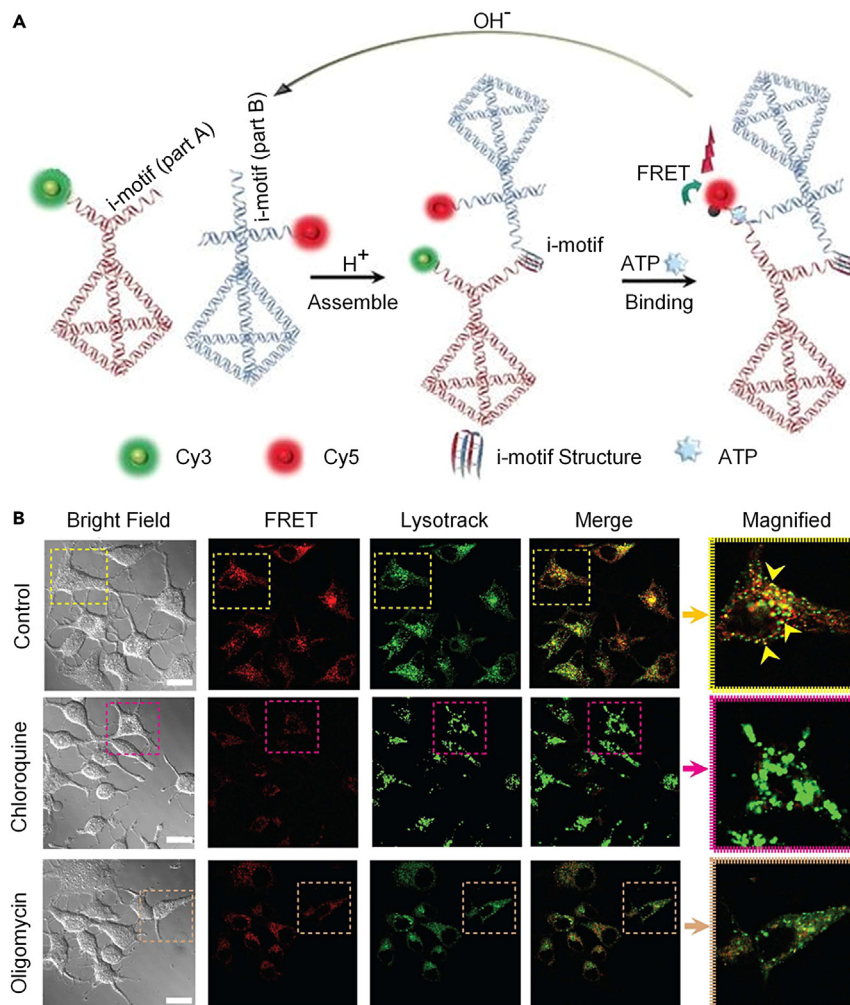


**Figure 3. Detection of ATP and adenosine triphosphate (ATP) levels in lysosomes based on DNA-guided intracellular self-assembly**

(A) Schematic of the intracellular self-assembly of two DNA tetrahedron probes via the sequential formation of i-motif structure and ATP aptamer in lysosomes, achieving detection through monitoring the efficiency of fluorescence resonance energy transfer between Cy3 and Cy5.

(B) Fluorescence microscopy images of the MCF-7 cells without treatment (control), treated with chloroquine and treated with oligomycin, respectively. Lysosomes were stained by LysoTrack. Scale bar: 20  $\mu\text{m}$ . Reprinted and adapted with permission from ref.<sup>10</sup>

way to regulate cell behaviors through intracellular DNA self-assembly, which can help us to deeply understand the subcellular structures and functions, provide insight into the mechanisms of drug action, and explore new targets in disease therapy. In this section, recent research on the regulation of cell behaviors through DNA self-assembly were introduced, and according to the methods of self-assembly, the research were divided into two parts, G-quadruplex-guided and i-motif-guided self-assembly.

In the G-quadruplex-guided DNA self-assembly, the guanine-rich DNA sequences were integrated into material systems to respond to intracellular high-level K<sup>+</sup> and form G-quadruplex structures.<sup>57,58</sup> Basu et al.<sup>11</sup> synthesized a thiolated conjugate of hyaluronic acid (HASH) grafted with guanine-rich ssDNA (HASH-DNA). The HASD-DNA chains were able to self-assemble into nanogels within cells through the formation of G-quadruplex structures. Basu et al.<sup>11</sup> found that the nanogels trapped inside the cytoplasm would cause the swelling and blebbing of cells, which was closely associated with cell oncosis, a special kind of non-apoptotic cell death mode. The results of microscopy images showed that at 1 h, the volume of the cells treated with HASH-DNA was 10-fold of the cells treated with the scrambled DNA-grafted HASH

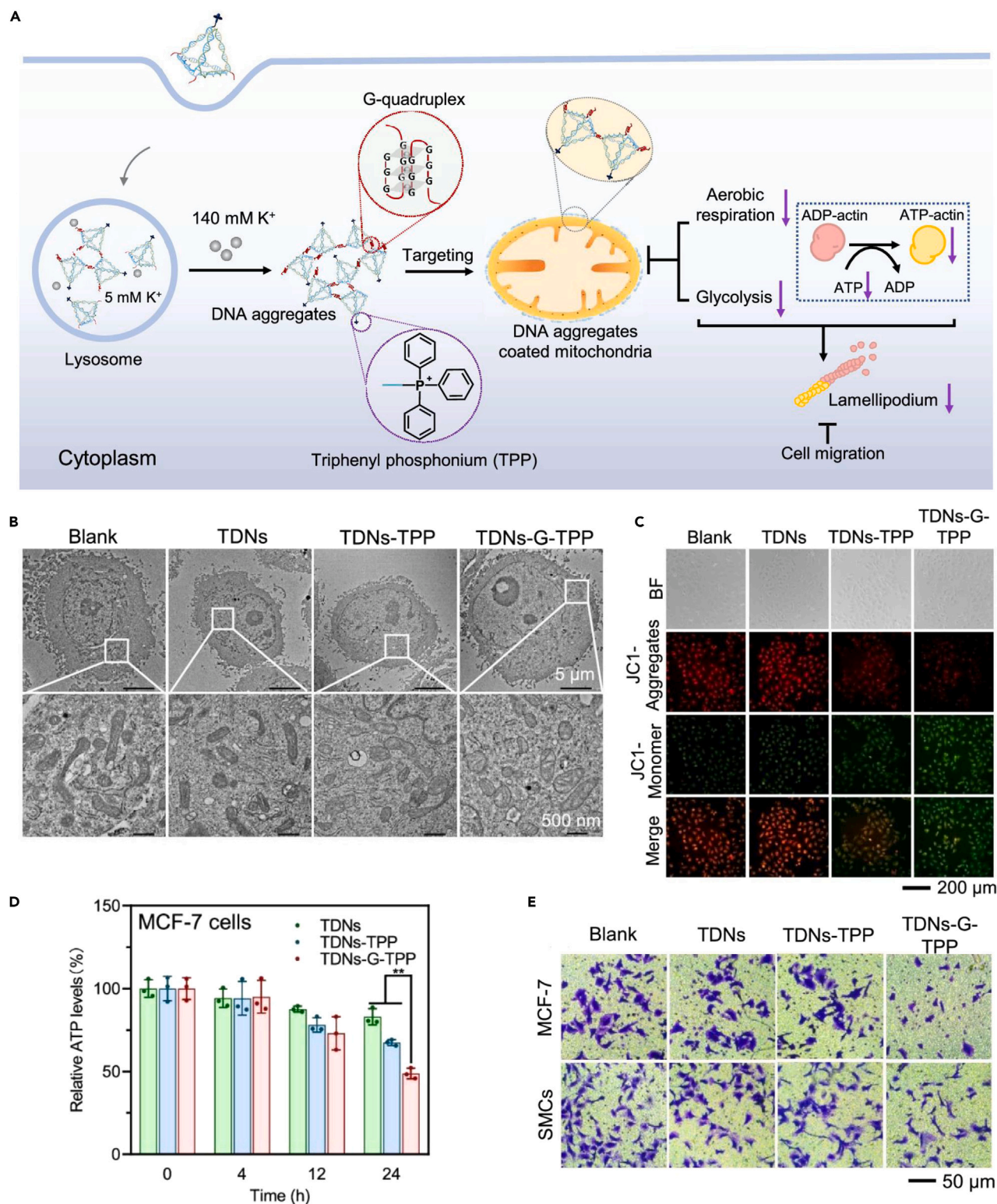


**Figure 4. Inhibition of mitochondrial functions through the intracellular self-assembly guided by G-quadruplex**

(A) Schematic of the self-assembly of G-rich DNA tetrahedron (TDN) modified with triphenylphosphine (TPP) on the surface of mitochondria, inhibiting the capability of mitochondria on ATP generation.

**Figure 4. Continued**

- (B) Bio-transmission electron microscopy images of MCF-7 cells treated with TDNs, TDNs-TPP, and TDNs-G-TPP, respectively.  
 (C) Fluorescence microscopy images showing mitochondrial membrane potential of MCF-7 cells measured with JC-1 assay kit.  
 (D) Intracellular ATP levels of MCF-7 cells with different treatments for 0, 4, 12, and 24 h, respectively. Data are presented as mean  $\pm$  SD, n = 3, \*\*p < 0.01.  
 (E) Transwell assay of the migration capability of MCF-7 cells and SMCs with different treatments for 48 h. Reprinted and adapted with permission from ref.<sup>14</sup>

(HASH-Mut). As the concentration of HASH-DNA increased, the viability of HeLa cells with HASH-DNA gradually decreased to 0%, while there was no significant change in the viability of cells with HASH-Mut compared with control groups, indicating that the G-quadruplex-guided intracellular self-assembly of HASH-DNA was able to influence the apoptosis of cells.

Yang et al.<sup>14</sup> designed a self-assembly strategy based on DNA tetrahedron (TDN) to influence the functions of mitochondria, thereby regulating the energy metabolism and migration behavior of cells (Figure 4A). The DNA tetrahedron was modified with triphenylphosphine (TPP) on one vertex, and the guanine (G)-rich sequence was designed on another vertex to form G-quadruplex under intracellular high-level  $K^+$ . Since TPP was able to target the surface of mitochondria, the self-assembly of DNA tetrahedrons occurred on the surface of mitochondria to form the DNA assembler. Since the dynamic division of mitochondria was inhibited by the coated DNA assembler, the morphology of mitochondria became swollen. The bio-transmission electron microscopy images demonstrated that the morphology of mitochondria in the MCF-7 cells treated with TDNs (without mitochondrial targeting) was similar to that in the control group, and the mitochondria treated with TDNs-TPP and TDNs-G-TPP were significantly enlarged (Figure 4B). On the other hand, the results of mitochondrial membrane potential in MCF-7 cells measured by JC-1 assay kit showed that the intensity ratio of red to green fluorescence in the TDNs-G-TPP group significantly decreased compared to the other groups (Figure 4C), indicating that the self-assembly of negatively charged DNA molecules efficiently decreased mitochondrial membrane potential. Yang et al. proposed that the negatively charged DNA assembler inhibited the glycolysis process by working as a barrier to the substrate communication of mitochondria, thus inhibiting aerobic respiration and ATP generation. The corresponding results were observed that the relative ATP level in the MCF-7 cells incubated with TDNs-G-TPP was significantly lower than that with other materials (Figure 4D). The lack of ATP impeded the formation of lamellipodium that was essential for the mobility of cells. Transwell assay demonstrated that the percentage of migrating cells in the TDNs-G-TPP group was higher than other material groups (Figure 4E), verifying that the migration capability of cells was inhibited due to the reduced ATP generation caused by the self-assembly of TDNs-G-TPP. Interestingly, compared to normal cells (SMCs), cancer cells (MCF-7) showed a significantly decreased capability to migrate (Figure 4E), which indicated that cancer cells were more vulnerable to mitochondrial interference.

In the i-motif-guided DNA self-assembly, the C-rich DNA sequences were integrated into material systems to respond to intracellular acidic environments, such as in lysosomes, and form i-motif structures.<sup>59</sup> Yang et al.<sup>13</sup> synthesized a double-stranded DNA with C-rich sticky ends (C-monomer) via polymerase chain reaction, during which 4',5',8'-Trimethylpsoralen was used to improve the thermal stability of DNA (Figure 5A). C-monomers were then compressed by high-concentration  $Mg^{2+}$  at pH 7.4 to nanoscale particles (C-nanoparticles), which was beneficial to improve the efficiency of cell internalization. In the acidic environment (pH~5.0) of lysosomes, C-nanoparticles dissociated to C-monomers again due to the weakened interactions between  $Mg^{2+}$  and DNA, and then C-monomers assembled into microhydrogel (DNA assembler) through the formation of i-motif structure. The *in vitro* experiments were performed to investigate the influence of the DNA self-assembly of C-nanoparticles on the cytoskeleton deformation, and the nanoparticles without C-rich sequences (NC-nanoparticles) were set up as control. U87GM cells were incubated with fluorophore (FAM)-labeled C-nanoparticles and NC-nanoparticles for 6 h, respectively, and then the F-actin cytoskeleton of cells was stained with RhB phalloidine. Fluorescence microscopy images showed that the DNA assembler with significant green fluorescence was observed in the cytoplasm of U87MG cells incubated with C-nanoparticles, and the F-actin filaments around the assembler were fragmentary; while in the cells incubated with NC-nanoparticles, the F-actin filaments were long and smooth, which was identical to that in untreated cells (Figure 5B). What's more, the analysis results of F-actin orientation showed that the orientation plots of untreated cells and NC-nanoparticle-treated cells showed monotonous color, indicating the highly consistent orientation of F-actin filaments; while the orientation plots of C-nanoparticle-treated cells showed more complex colors (Figure 5B), indicating the reorganization of F-actin filaments. It was proved that the self-assembly of C-nanoparticles promoted the dynamic organization of F-actin, subsequently leading to cytoskeleton deformation. Cytoskeleton was closely associated

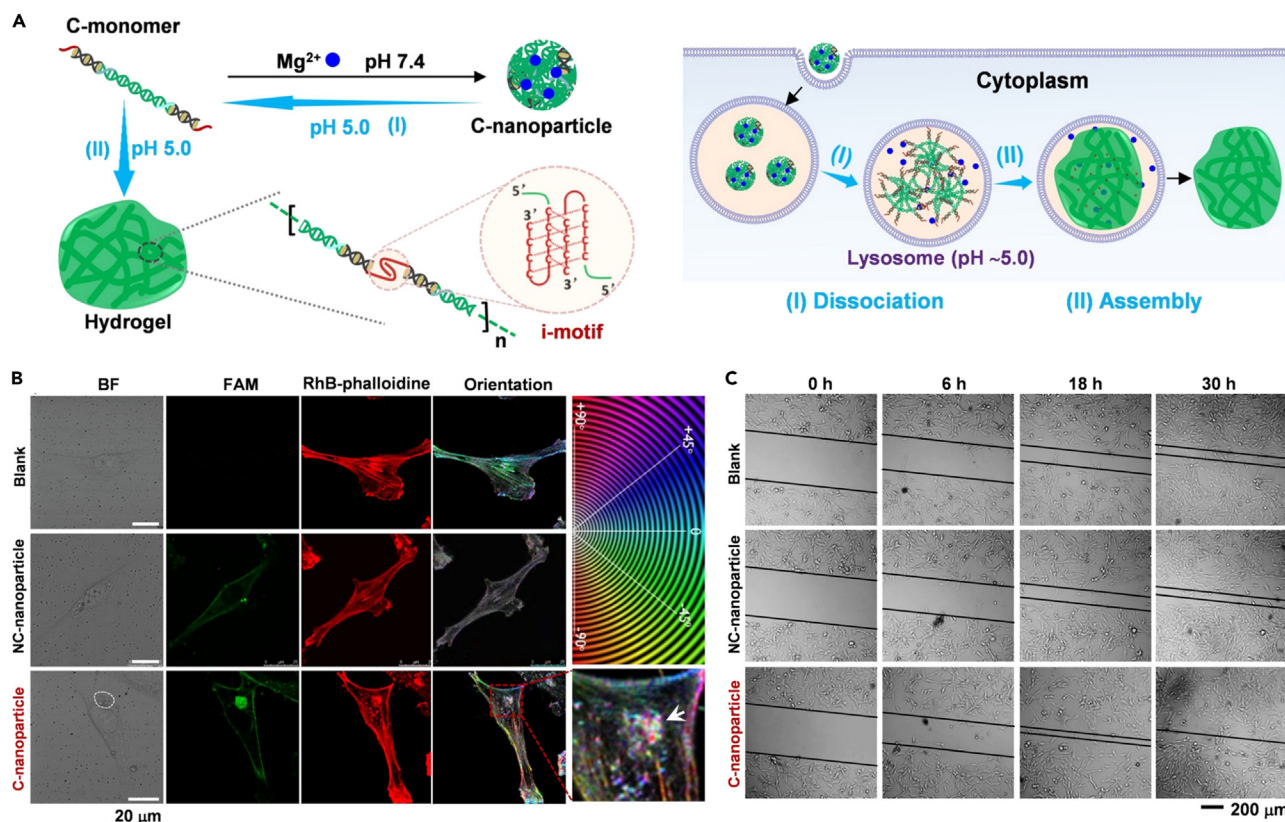


**Figure 5. Cytoskeleton deformation through the intracellular self-assembly guided by i-motif structure**

(A) Schematic of the intracellular self-assembly of C-nanoparticles through dissociation and reassembly in lysosomes.

(B) Fluorescence microscopy images and corresponding orientation plots of the U87MG cells incubated with FAM-labeled C-nanoparticles and NC-nanoparticles for 6 h, respectively.

(C) Microscopy images of cell scratch experiment, in which U87MG cells were incubated with C-nanoparticles and NC-nanoparticles for different times, respectively. Reprinted and adapted with permission from ref.<sup>13</sup>

with the migration ability of cells. Consequently, cell scratch experiments were performed to investigate the migration ability of cells, and the results showed that the healing rate of scratch in the C-nanoparticle group was faster than that in the NC-nanoparticle group, and reached 100% in 30 h (Figure 5C), demonstrating that the i-motif-guided self-assembly of C-nanoparticles was able to promote cell migration through deforming cytoskeleton.

To further investigate the regulation of this i-motif-guided DNA self-assembly on cell behaviors, Yang et al.<sup>14</sup> developed a C-rich DNA nanoframework based on polymeric N-Isopropyl acrylamide (NDHi) (Figures 6A and 6B). First, they measured the activity of tartrate-resistant acid phosphatase (TRAP), a lysosomal enzyme to hydrolyze phosphoric acid bonds at pH 5.0-6.0, to explore the lysosomal interference caused by the self-assembly. The activity of TRAP was by naphthol-diazonium salt coupling method, and the DNA nanoframework without C-rich sequence (NDHni) was set up as control. The analysis results showed that the color of A549 cells incubated with NDHi was significantly deeper than that incubated with NDHni (Figure 6C), indicating that the activity of TRAP was weakened by the i-motif-guided self-assembly of NDHi. Yang et al. thought that the i-motif-guided self-assembly consumed the H<sup>+</sup> in lysosomes, which reduced the lysosomal acidity and thus weakened the activity of TRAP. The weakened activity of TRAP would reduce the degradation of DNA/RNA in lysosomes, and Yang et al. demonstrated it by investigating the gene silencing efficiency of siActin that specifically downregulated β-actin expression. There were six groups of A549 cells with different treatments, including PBS buffer, NDHi loaded with scramble siRNA chain (NDHi-siScram), lipo-transfected siActin that specifically downregulated β-actin expression (Lipo), NDHni-siActin, NDHni-siActin with chloroquine pretreatment (NDHni+CQ), and NDHi-siActin, in which chloroquine was used to increase the pH value in lysosomes. After analyzing the fluorescence

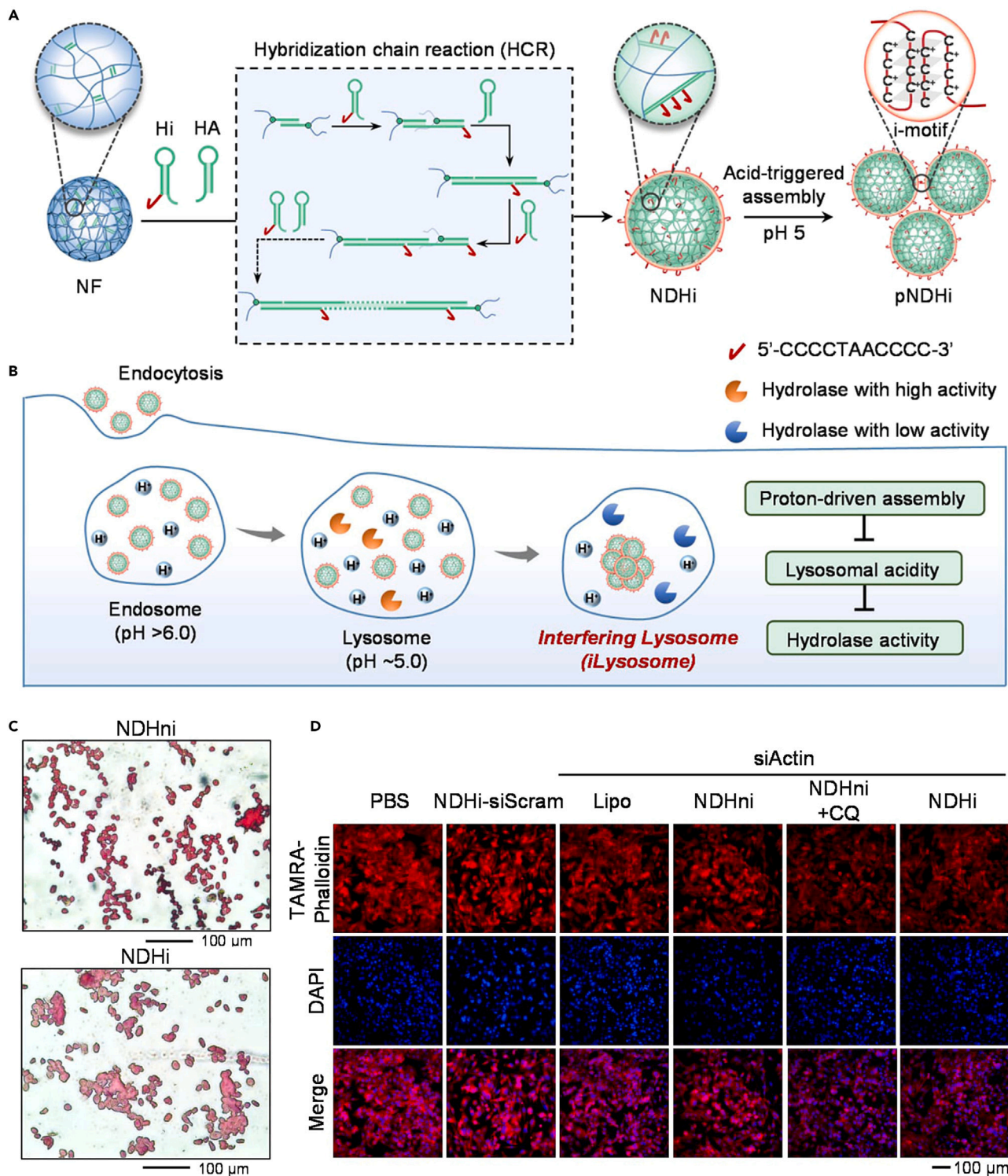


**Figure 6. Lysosome interference through the intracellular self-assembly guided by i-motif structure**

(A) Synthesis of C-rich DNA nanoframeworks (DNHi) through integrating C-rich DNA hairpin (Hi) into DNA nanoframes (NF) through the HCR between Hi and another DNA hairpin (HA).

(B) Schematic of the intracellular self-assembly of DNHi in lysosomes, reducing the lysosomal acidity and thus weakening the activity of lysosomal hydrolase.

Microscopy images (C) of tartrate-resistant acid phosphatase staining of A549 cells treated with different materials for 4 h. Fluorescence microscopy images (D) of the TAMRA-stained  $\beta$ -actin in A549 cells treated with different materials. siActin was able to specifically downregulate  $\beta$ -actin expression. siScram was the scramble siRNA that didn't regulate protein expression. Reprinted and adapted with permission from ref.<sup>12</sup>

intensity of stained  $\beta$ -actin in cells, the results showed that the fluorescence intensity in the NDHi-siActin group was significantly lower than that in the NDHni-siActin group, and similar to that in the chloroquine pretreatment group (Figure 6D), indicating that the siActin loaded by NDHi was efficiently protected from the degradation of hydrolase. These results suggested that i-motif-guided DNA self-assembly was able to weaken the activity of lysosomal hydrolase by reducing the lysosomal acidity.

On the basis of preceding research, Yang et al.<sup>15</sup> introduced ceria into the i-motif-guided DNA self-assembly system to construct artificial peroxisome (AP) for the scavenging of high-level reactive oxygen species (ROS) in cells (Figure 7A). In the material synthesis, C-rich branched DNA was utilized to form the primary DNA assembler (DAS) that interacted with ceria to form DNA-ceria nanocomplex (DCNC); during cell internalization, DCNC dissociated in early endosomes (pH $\sim$ 6.5), and then reassembled into the secondary DNA assembler (AP) through the formation of i-motif; the self-assembly process in lysosomes prolonged the retention time of AP in cells, thus enhancing the efficiency of the ceria in AP to scavenge ROS (Figure 7A). The fluorescent probes to ROS were used to evaluate the efficiency of ROS scavenging, and the materials without C-rich sequences (D<sub>ni</sub>AS and D<sub>ni</sub>CNC) were set up as control. The results showed that the fluorescence intensity in the DCNC group was significantly lower than the other groups, especially D<sub>ni</sub>CNC, indicating that the self-assembly improved the efficiency of ROS scavenging (Figure 7B). In the cells with oxidative stress, the functions of mitochondria were inhibited due to intracellular high-level ROS, thus resulting in weakened mobility and accelerated irreversible apoptosis of cells. Transwell experiments were performed to evaluate the mobility of cells with different materials, and compared to other groups, the mobility of MCF-7 cells was significantly recovered after incubation with DCNC (Figure 7C). The living/dead cell assay also confirmed that the percentage of living cells in the DCNC group was significantly higher than that in other groups (Figure 7D). These results demonstrated that the i-motif-guided DNA self-assembly with ceria was able to regulate the mobility and apoptosis of MCF-7 cells.

### Conclusions and outlooks

In this review, we focused on the intracellular self-assembly methods based on the conformational transition of DNA molecules and introduced the applications for the detection of intracellular biomolecules and the regulation of cell behaviors. In the self-assembly systems, the specific conformational transition of DNA mainly relied on the heterogeneity between different cells or at the subcellular level, such as the concentration difference of metal ions (K<sup>+</sup>), biomolecules (ATP, mRNA, and miRNA), and proton. In the detection of intracellular biomolecules, the self-assembly systems were designed to be triggered by target molecules with high specificity and ensure efficient enhancement or weakening of target signals, thus reducing the influence of non-target factors on detection results. In particular, the properties of complementary base pairing endowed DNA molecules with natural advantages to recognize intracellular RNA with high specificity or use RNA as the initiator to trigger self-assembly, which improved the applicability of DNA self-assembly in the investigations on intracellular RNA. As to the regulation of cell behaviors, the self-assembly process was usually designed to interfere intracellular environment by consuming biofunctional molecules, applying physical pressure or blocking substance exchange, and the regulation mechanism was investigated via monitoring the change of cell behaviors and corresponding biomarkers.

At present, the studies on DNA-guided intracellular self-assembly are still in the starting stage, and there are still challenges to solve. 1) The stability of DNA assembly precursor is challenged by various nucleases in biological environments. In particular, compared with detection, the regulation of cell behaviors demands the DNA assembler to stay longer in cells, to exert its functions. As mentioned in this review, scientists have improved the stability of DNA materials by carrier (liposome, ZnO), covalent modification, and metal ion compression, and the topological transformation after self-assembly has been also proved to achieve the longer retention time of DNA assembler in cells. In future studies, especially *in vivo* studies, the stability, delivery efficiency, and assembly strategy of DNA units in more complex physiological environments should be considered more detailly. 2) To the self-assembly strategies triggered by target DNA/RNA, such as HCR, sequence design is essential to avoid the unexpected assembly that is triggered by the non-target molecules with the similar sequences to target molecules in cells, ensuring the high specificity of self-assembly. 3) The self-assembly efficiency of monomers in living cells is essential for the following applications, which may be optimized by improving the cellular uptake efficiency of monomers or choosing more stable self-assembly strategies. 4) It is promising to use other molecules-triggered intracellular DNA self-assembly to develop more detection methods of disease-related biomarkers, such as enzyme-triggered self-assembly, or aptamer-guided self-assembly that is triggered by the target of aptamer. It

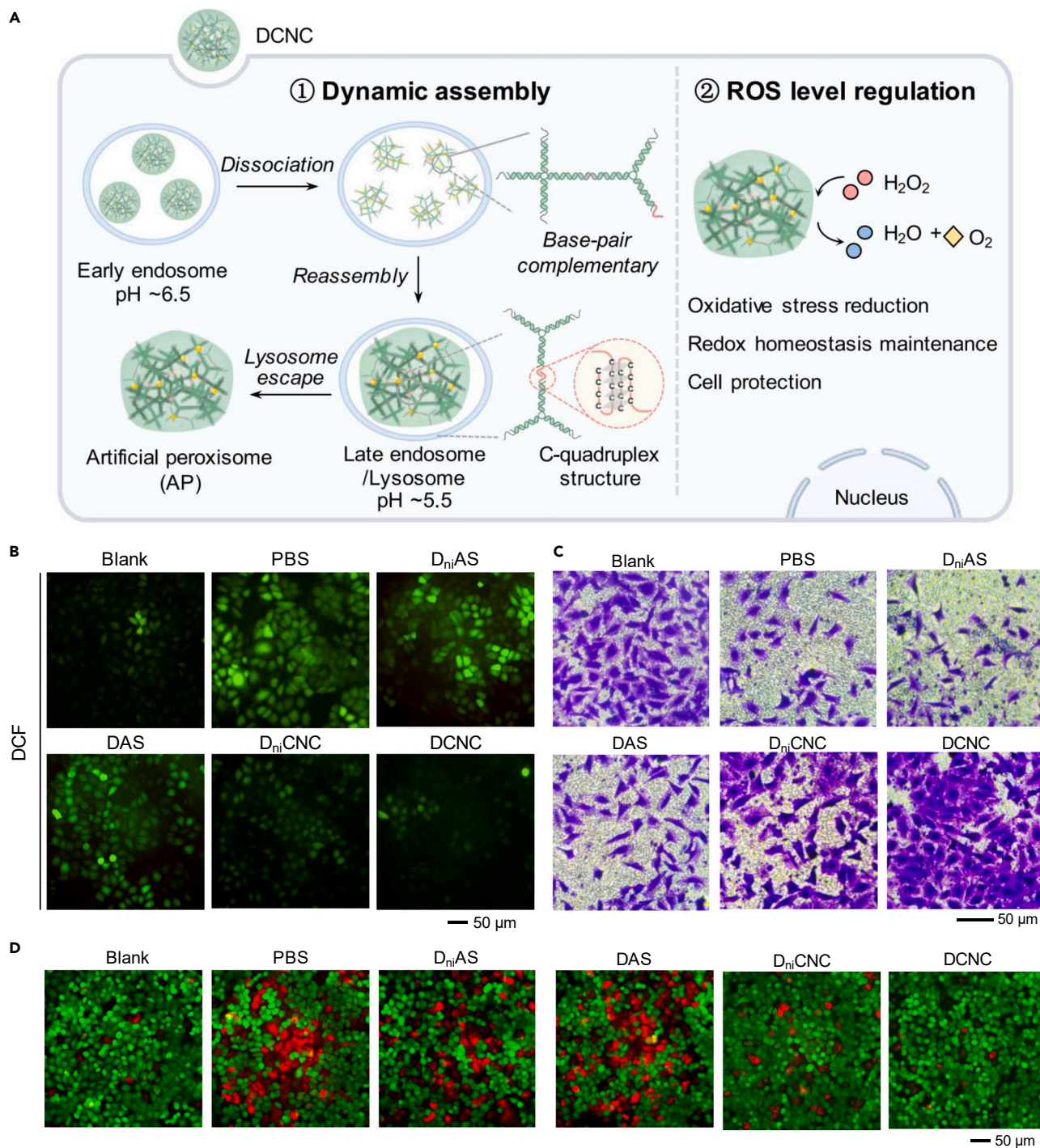


**Figure 7. Regulation of reactive oxygen species (ROS) level through the intracellular self-assembly guided by i-motif structure**

(A) Schematic of the intracellular self-assembly of C-rich branched DNA and ceria in lysosomes to construct artificial peroxisome (AP), efficiently scavenging the intracellular high-level ROS.

(B) Fluorescence microscopy images showing the ROS levels in MCF-7 cells after incubation with different materials.

(C) Microscopy images of MCF-7 cells treated with different materials in transwell invasion assay.

(D) Fluorescence microscopy images of the MCF-7 cells treated with different materials in living/dead cell assay. Reprinted and adapted with permission from ref.<sup>15</sup>

is noticed that the stability of self-assembly structures should support the formation of self-assembler in cells, which is essential to address the problems of signal leakage and false positives in detection applications. 5) The mechanism to regulate cell behaviors by DNA-guided intracellular self-assembly may be from a common result induced by charge transfer, space interference, and matter consumption, which is not fully understood. We envision that this review can attract more attention on the DNA-guided intracellular self-assembly, and with in-depth studies, the self-assembly strategy can provide a new way to explore the mechanism and treatment of major diseases.

## ACKNOWLEDGMENTS

This work was supported by National Natural Science Foundation of China (grant no. 22225505).

## REFERENCES

- Whitesides, G.M., and Grzybowski, B. (2002). Self-assembly at all scales. *Science* 295, 2418–2421.
- Suzuki, Y., Endo, M., and Sugiyama, H. (2015). Lipid-bilayer-assisted two-dimensional self-assembly of DNA origami nanostructures. *Nat. Commun.* 6, 8052.
- Wang, H., Feng, Z., and Xu, B. (2017). Bioinspired assembly of small molecules in cell milieu. *Chem. Soc. Rev.* 46, 2421–2436.
- Banani, S.F., Lee, H.O., Hyman, A.A., and Rosen, M.K. (2017). Biomolecular condensates: organizers of cellular biochemistry. *Nat. Rev. Mol. Cell Biol.* 18, 285–298.
- He, P.P., Li, X.D., Wang, L., and Wang, H. (2019). Bispirene-based self-assembled nanomaterials: in vivo self-assembly, transformation, and biomedical effects. *Acc. Chem. Res.* 52, 367–378.
- Li, L.L., Qiao, Z.Y., Wang, L., and Wang, H. (2019). Programmable construction of peptide-based materials in living subjects: from modular design and morphological control to theranostics. *Adv. Mater.* 31, e1804971.
- Fang, C., Li, Y., Hu, S., Wang, H., Chen, X., and Zhu, X. (2021). Self-assembled growing DNA tree mediated by exosomes for amplified imaging of messenger RNA in living cells. *Anal. Chem.* 93, 8414–8422.
- He, D., He, X., Yang, X., and Li, H.W. (2017). A smart ZnO@polydopamine-nucleic acid nanosystem for ultrasensitive live cell mRNA imaging by the target-triggered intracellular self-assembly of active DNAzyme nanostructures. *Chem. Sci.* 8, 2832–2840.
- Liu, R., Zhang, S., Zheng, T.T., Chen, Y.R., Wu, J.T., and Wu, Z.S. (2020). Intracellular nonenzymatic in situ growth of three-dimensional DNA nanostructures for imaging specific biomolecules in living cells. *ACS Nano* 14, 9572–9584.
- Peng, P., Du, Y., Zheng, J., Wang, H., and Li, T. (2019). Reconfigurable bioinspired framework nucleic acid nanoplateform dynamically manipulated in living cells for subcellular imaging. *Angew. Chem. Int. Ed.* 58, 1648–1653.
- Beals, N., Model, M.A., Worden, M., Hegmann, T., and Basu, S. (2018). Intermolecular G-quadruplex induces hyaluronic acid-DNA superpolymers causing cancer cell swelling, blebbing, and death. *ACS Appl. Mater. Inter.* 10, 6869–6878.
- Dong, Y., Li, F., Lv, Z., Li, S., Yuan, M., Song, N., Liu, J., and Yang, D. (2022). Lysosome interference enabled by proton-driven dynamic assembly of DNA nanoframeworks inside cells. *Angew. Chem. Int. Ed.* 61, e202207770.
- Guo, X., Li, F., Liu, C., Zhu, Y., Xiao, N., Gu, Z., Luo, D., Jiang, J., and Yang, D. (2020). Construction of organelle-like architecture by dynamic DNA assembly in living cells. *Angew. Chem. Int. Ed.* 59, 20651–20658.
- Li, F., Liu, Y., Dong, Y., Chu, Y., Song, N., and Yang, D. (2022). Dynamic assembly of DNA nanostructures in living cells for mitochondrial interference. *J. Am. Chem. Soc.* 144, 4667–4677.
- Yao, C., Xu, Y., Tang, J., Hu, P., Qi, H., and Yang, D. (2022). Dynamic assembly of DNA-ceria nanocomplex in living cells generates artificial peroxisome. *Nat. Commun.* 13, 7739.
- Huber, M.C., Schreiber, A., von Olshausen, P., Varga, B.R., Kretz, O., Joch, B., Barnert, S., Schubert, R., Eimer, S., Kele, P., and Schiller, S.M. (2015). Designer amphiphilic proteins as building blocks for the intracellular formation of organelle-like compartments. *Nat. Mater.* 14, 125–132.
- He, H., Tan, W., Guo, J., Yi, M., Shy, A.N., and Xu, B. (2020). Enzymatic noncovalent synthesis. *Chem. Rev.* 120, 9994–10078.
- Tan, W., Zhang, Q., Wang, J., Yi, M., He, H., and Xu, B. (2021). Enzymatic assemblies of thiophosphopeptides instantly target golgi apparatus and selectively kill cancer cells. *Angew. Chem. Int. Ed.* 60, 12796–12801.
- Yang, Z., Liang, G., Guo, Z., Guo, Z., and Xu, B. (2007). Intracellular hydrogelation of small molecules inhibits bacterial growth. *Angew. Chem. Int. Ed.* 46, 8216–8219.
- Wei, S.P., Qian, Z.G., Hu, C.F., Pan, F., Chen, M.T., Lee, S.Y., and Xia, X.X. (2020). Formation and functionalization of membraneless compartments in *Escherichia coli*. *Nat. Chem. Biol.* 16, 1143–1148.
- Dergham, M., Lin, S., and Geng, J. (2022). Supramolecular self-assembly in living cells. *Angew. Chem. Int. Ed.* 61, e202114267.
- Liu, Q., Wang, D., Yuan, M., He, B.F., Li, J., Mao, C., Wang, G.S., and Qian, H. (2018). Capturing intracellular oncogenic microRNAs with self-assembled DNA nanostructures for microRNA-based cancer therapy. *Chem. Sci.* 9, 7562–7568.
- Delebecque, C.J., Lindner, A.B., Silver, P.A., and Aldaye, F.A. (2011). Organization of intracellular reactions with rationally designed RNA assemblies. *Science* 333, 470–474.
- Qi, X., Liu, X., Matiski, L., Rodriguez Del Villar, R., Yip, T., Zhang, F., Sokalingam, S., Jiang, S., Liu, L., Yan, H., and Chang, Y. (2020). RNA origami nanostructures for potent and safe anticancer immunotherapy. *ACS Nano* 14, 4727–4740.
- Gu, C., Zhang, T., Lv, C., Liu, Y., Wang, Y., and Zhao, G. (2020). His-mediated reversible self-assembly of ferritin nanocages through two different switches for encapsulation of cargo molecules. *ACS Nano* 14, 17080–17090.
- Myhrvold, C., Baym, M., Hanikel, N., Ong, L.L., Gootenberg, J.S., and Yin, P. (2017). Barcode extension for analysis and reconstruction of structures. *Nat. Commun.* 8, 14698.
- Nie, Z., Petukhova, A., and Kumacheva, E. (2010). Properties and emerging applications of self-assembled structures made from inorganic nanoparticles. *Nat. Nanotechnol.* 5, 15–25.
- Wang, J., Chao, J., Liu, H., Su, S., Wang, L., Huang, W., Willner, I., and Fan, C. (2017). Clamped hybridization chain reactions for the self-assembly of patterned DNA hydrogels. *Angew. Chem. Int. Ed.* 56, 2171–2175.
- Li, F., Yu, W., Zhang, J., Dong, Y., Ding, X., Ruan, X., Gu, Z., and Yang, D. (2021). Spatiotemporally programmable cascade hybridization of hairpin DNA in polymeric nanoframework for precise siRNA delivery. *Nat. Commun.* 12, 1138.
- Dong, Y., Yao, C., Zhu, Y., Yang, L., Luo, D., and Yang, D. (2020). DNA functional materials assembled from branched DNA: design, synthesis, and applications. *Chem. Rev.* 120, 9420–9481.
- Li, F., Tang, J., Geng, J., Luo, D., and Yang, D. (2019). Polymeric DNA hydrogel: design, synthesis and applications. *Prog. Polym. Sci.* 98, 101163.

32. Li, F., Lv, Z., Zhang, X., Dong, Y., Ding, X., Li, Z., Li, S., Yao, C., and Yang, D. (2021). Supramolecular self-assembled DNA nanosystem for synergistic chemical and gene regulations on cancer cells. *Angew. Chem. Int. Ed.* *60*, 25557–25566.
33. Sun, S., Xu, H., Yang, Y., Wang, L., Ye, L., Jiang, H., Xue, C., Shen, Z., and Wu, Z.-S. (2022). Intracellular in situ assembly of palindromic DNA hydrogel for predicting malignant invasion and preventing tumorigenesis. *Chem. Eng. J.* *428*, 131150. <https://doi.org/10.1016/j.cej.2021.131150>.
34. Shi, Z., Zhang, X., Cheng, R., Li, B., and Jin, Y. (2016). Sensitive detection of intracellular RNA of human telomerase by using graphene oxide as a carrier to deliver the assembly element of hybridization chain reaction. *Analyst* *141*, 2727–2732.
35. Zhang, P., Ouyang, Y., Sohn, Y.S., Fadeev, M., Karmi, O., Nechushtai, R., Stein, I., Pikarsky, E., and Willner, I. (2022). miRNA-Guided imaging and photodynamic therapy treatment of cancer cells using Zn(II)-protoporphyrin IX-loaded metal-organic framework nanoparticles. *ACS Nano* *16*, 1791–1801.
36. Rakers, V., Cadinu, P., Edel, J.B., and Vilar, R. (2018). Development of microfluidic platforms for the synthesis of metal complexes and evaluation of their DNA affinity using online FRET melting assays. *Chem. Sci.* *9*, 3459–3469.
37. Summers, P.A., Lewis, B.W., Gonzalez-Garcia, J., Porreca, R.M., Lim, A.H.M., Cadinu, P., Martin-Pintado, N., Mann, D.J., Edel, J.B., Vannier, J.B., et al. (2021). Visualising G-quadruplex DNA dynamics in live cells by fluorescence lifetime imaging microscopy. *Nat. Commun.* *12*, 162.
38. Biffi, G., Tannahill, D., McCafferty, J., and Balasubramanian, S. (2013). Quantitative visualization of DNA G-quadruplex structures in human cells. *Nat. Chem.* *5*, 182–186.
39. Hur, J.H., Kang, C.Y., Lee, S., Parveen, N., Yu, J., Shamim, A., Yoo, W., Ghosh, A., Bae, S., Park, C.J., and Kim, K.K. (2021). AC-motif: a DNA motif containing adenine and cytosine repeat plays a role in gene regulation. *Nucleic Acids Res.* *49*, 10150–10165.
40. Iaccarino, N., Cheng, M., Qiu, D., Pagano, B., Amato, J., Di Porzio, A., Zhou, J., Randazzo, A., and Mergny, J.L. (2021). Effects of sequence and base composition on the CD and TDS profiles of i-DNA. *Angew. Chem. Int. Ed.* *60*, 10295–10303.
41. Park, H., Kim, J., Jung, S., and Kim, W.J. (2018). DNA-Au nanomachine equipped with i-motif and G-quadruplex for triple combinatorial anti-tumor therapy. *Adv. Funct. Mater.* *28*, 1705416.
42. Wu, L., Wang, Y., Xu, X., Liu, Y., Lin, B., Zhang, M., Zhang, J., Wan, S., Yang, C., and Tan, W. (2021). Aptamer-based detection of circulating targets for precision medicine. *Chem. Rev.* *121*, 12035–12105.
43. Wu, C., Han, D., Chen, T., Peng, L., Zhu, G., You, M., Qiu, L., Sefah, K., Zhang, X., and Tan, W. (2013). Building a multifunctional aptamer-based DNA nanoassembly for targeted cancer therapy. *J. Am. Chem. Soc.* *135*, 18644–18650.
44. Li, J., Zheng, C., Cansiz, S., Wu, C., Xu, J., Cui, C., Liu, Y., Hou, W., Wang, Y., Zhang, L., et al. (2015). Self-assembly of DNA nanohydrogels with controllable size and stimuli-responsive property for targeted gene regulation therapy. *J. Am. Chem. Soc.* *137*, 1412–1415.
45. Li, Q., Liu, L., Mao, D., Yu, Y., Li, W., Zhao, X., and Mao, C. (2020). ATP-triggered, allosteric self-assembly of DNA nanostructures. *J. Am. Chem. Soc.* *142*, 665–668.
46. Zhan, P., Jahnke, K., Liu, N., and Göpfrich, K. (2022). Functional DNA-based cytoskeletons for synthetic cells. *Nat. Chem.* *14*, 958–963.
47. Sun, Y., and Li, T. (2018). Composition-tunable hollow Au/Ag SERS nanoprobe coupled with target-catalyzed hairpin assembly for triple-amplification detection of miRNA. *Anal. Chem.* *90*, 11614–11621.
48. Li, C., Xue, C., Wang, J., Luo, M., Shen, Z., and Wu, Z.S. (2019). Oriented tetrahedron-mediated protection of catalytic DNA molecular-scale detector against in vivo degradation for intracellular miRNA detection. *Anal. Chem.* *91*, 11529–11536.
49. Fan, Z., Zhao, J., Chai, X., and Li, L. (2021). A cooperatively activatable, DNA-based fluorescent reporter for imaging of correlated enzymatic activities. *Angew. Chem. Int. Ed.* *60*, 14887–14891.
50. Cheng, H., Liu, J., Ma, W., Duan, S., Huang, J., He, X., and Wang, K. (2018). Low background cascade signal amplification electrochemical sensing platform for tumor-related mRNA quantification by target-activated hybridization chain reaction and electroactive cargo release. *Anal. Chem.* *90*, 12544–12552.
51. Wei, Q., Liu, H., Zhou, H., Zhang, D., Zhang, Z., and Zhou, Q. (2015). Anticancer activity of a thymidine quinoxaline conjugate is modulated by cytosolic thymidine pathways. *BMC Cancer* *15*, 159.
52. Nazari, M., Gargari, S.L.M., Sahebghadam Lotfi, A., Rassaei, M.J., and Taheri, R.A. (2019). Aptamer-based sandwich assay for measurement of thymidine kinase 1 (TK1) in serum of cancerous patients. *Biochemistry* *58*, 2373–2383.
53. Qiu, W., Wang, Z., Chen, R., Shi, H., Ma, Y., Zhou, H., Li, M., Li, W., Chen, H., and Zhou, H. (2020). Xiaoi jiedu recipe suppresses hepatocellular carcinogenesis through the miR-200b-3p/Notch1 axis. *Cancer Manag. Res.* *12*, 11121–11131.
54. Liu, H., Li, Q., Li, M., Ma, S., and Liu, D. (2017). In situ hot-spot assembly as a general strategy for probing single biomolecules. *Anal. Chem.* *89*, 4776–4780.
55. Chen, Z., Xie, Y., Huang, W., Qin, C., Yu, A., and Lai, G. (2019). Exonuclease-assisted target recycling for ultrasensitive electrochemical detection of microRNA at vertically aligned carbon nanotubes. *Nanoscale* *11*, 11262–11269.
56. Dong, H., Lei, J., Ding, L., Wen, Y., Ju, H., and Zhang, X. (2013). MicroRNA: function, detection, and bioanalysis. *Chem. Rev.* *113*, 6207–6233.
57. Xiao, F., Chen, Z., Wei, Z., and Tian, L. (2020). Hydrophobic interaction: a promising driving force for the biomedical applications of nucleic acids. *Adv. Sci.* *7*, 2001048.
58. Lee, D.S.M., Ghanem, L.R., and Barash, Y. (2020). Integrative analysis reveals RNA G-quadruplexes in UTRs are selectively constrained and enriched for functional associations. *Nat. Commun.* *11*, 527.
59. Gao, B., Zheng, Y.T., Su, A.M., Sun, B., Xi, X.G., and Hou, X.M. (2022). Remodeling the conformational dynamics of I-motif DNA by helicases in ATP-independent mode at acidic environment. *iScience* *25*, 103575.